

# Ramsey interferometry with guided ultracold atoms

D. Seidel<sup>a</sup> and J.G. Muga

Departamento de Química-Física, Universidad del País Vasco, Apartado Postal 644, 48080 Bilbao, Spain

Received 4 April 2006

Published online 13 September 2006 – © EDP Sciences, Società Italiana di Fisica, Springer-Verlag 2006

**Abstract.** We examine the passage of ultracold two-level atoms in a waveguide through two separated laser fields for the nonresonant case. We show that implications of the atomic quantised motion change dramatically the behaviour of the interference fringes compared to the semiclassical description of this optical Ramsey interferometer. Using two-channel recurrence relations we are able to express the double-laser scattering amplitudes by means of the single-laser ones and to give explicit analytical results. When considering slower and slower atoms, the transmission probability of the system changes considerably from an interference behaviour to a regime where scattering resonances prevail. This may be understood in terms of different families of trajectories that dominate the overall transmission probability in the weak field or in the strong field limit.

**PACS.** 42.50.Ct Quantum description of interaction of light and matter; related experiments – 03.75.-b Matter waves – 39.20.+q Atom interferometry techniques

## 1 Introduction

Atom interferometry based on Ramsey’s method with separated fields [1] is an important tool of modern precision measurements. A basic feature of the observed Ramsey interference fringes is that its width is simply the inverse of the time taken by the atoms to cross the intermediate region. For precision measurement purposes, as in atomic clocks, this implicates the desire for very slow (ultracold) atoms. Experimentally, atomic velocities of the order of 1 cm/s are within discussion for space-based atomic clocks [2]. But, if the kinetic energy becomes comparable with the atom-field interaction energy, one has to take into account the quantised centre-of-mass motion of the atom and the well-known semiclassical results have to be corrected. Recoil effects have been studied in detail by Bordé and co-workers [3]. The quantum reflections due to the field have first been considered for ultracold atoms passing through one [4] or two [5] resonant micromaser cavities. The nonresonant case has been investigated so far only for one field zone with interesting consequences for the induced emission process inside the cavity [6].

In this letter we study the interference fringes with respect to detuning for ultracold atoms passing through two separated laser fields, taking into account reflection effects based on quantised longitudinal motion. In general, optical Ramsey interferometry has to be performed with at least three laser beams to avoid the spatial separation of the internal states due to transverse momentum transfer [7]. However, we propose to direct the atoms in a narrow waveguide and to work in a regime for which excitation of the transversal modes may be neglected.

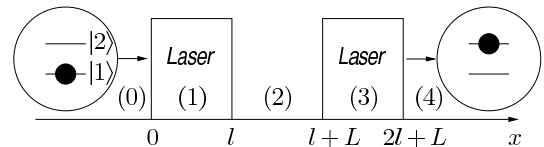


**Fig. 1.** Scheme of the optical Ramsey atom interferometer. The regions with constant potential are labeled by  $m = 0, \dots, 4$ , respectively.

For waveguides of width  $a = 100$  nm [8] and for caesium the energy gap to the first transversally excited state is  $\delta E = 2\pi\hbar \times 0.113$  MHz. Now, a minor modification of reference [9] to incorporate detuning shows that excitation mainly occurs at the “Rabi resonances”  $\hbar(\Omega^2 + \Delta^2)^{1/2} = \delta E$ , where  $\Omega$  is the Rabi frequency and  $\Delta = \omega_L - \omega_{12}$  denotes the detuning between laser frequency and atomic transition frequency. For Rabi frequencies of the order of  $2\pi \times 0.016$  MHz one would have a detuning range  $\Delta \approx 2\pi \times (-0.11 \dots 0.11)$  MHz for which transversal excitation can be neglected. However, it must be borne in mind that the laser changes the longitudinal atomic momentum since it acts as a quantum mechanical potential, even for  $\Delta = 0$  [10]. For convenience we restrict our analysis to classical fields, but we emphasise the fact that our results can be easily carried over to the case of two quantised fields (maser physics) by using the appropriate single-cavity scattering coefficients given in reference [6].

## 2 Model

We consider the basic Ramsey setup where a two-level atom initially in the ground state moves along the  $x$ -axis

<sup>a</sup> e-mail: dirk.seidel@ehu.es

on the way to two separated oscillating fields localised between 0 and  $l$  and between  $l + L$  and  $2l + L$  (Fig. 1). The measured quantity is the transmission probability of excited atoms,  $P_{12}$ , as a function of the laser detuning  $\Delta$ . In the interaction picture and using the dipole and rotating-wave approximation, the effective 1D system in the transversal ground state of the waveguide may be described by the Hamiltonian

$$H = \frac{\hat{p}^2}{2m} - \hbar\Delta|2\rangle\langle 2| + \frac{\hbar}{2}\Omega(\hat{x})(|1\rangle\langle 2| + |2\rangle\langle 1|), \quad (1)$$

where the first term is the kinetic energy of the atom and  $\Omega(x)$  is the position-dependent Rabi frequency. For the explicit  $x$  dependence we assume for simplicity mesa functions throughout this paper,  $\Omega(x) = \Omega$  for  $x \in [0, l]$  and  $x \in [l + L, 2l + L]$  and zero elsewhere. The physical picture and main conclusions do not depend critically on this form.

In order to derive  $P_{12}$  one has to solve the stationary Schrödinger equation (SSE),  $H\Phi_k = E_k\Phi_k$ , with  $E_k = \hbar^2k^2/2m$  and  $\Phi_k = \phi_k^{(1)}|1\rangle + \phi_k^{(2)}|2\rangle$ . This is easy in the semiclassical regime where  $E_k \gg \hbar\Omega, \hbar\Delta$  and the centre-of-mass motion can be treated independently of the internal dynamics. In this regime and with the effective Rabi frequency  $\Omega' = \sqrt{\Omega^2 + \Delta^2}$  one obtains [1]

$$P_{12}^{\text{scl}} = \frac{4\Omega^2}{\Omega'^2} \sin^2\left(\frac{m\Omega'l}{2\hbar k}\right) \left[ \cos\left(\frac{m\Delta L}{2\hbar k}\right) \cos\left(\frac{m\Omega'l}{2\hbar k}\right) - \frac{\Delta}{\Omega'} \sin\left(\frac{m\Delta L}{2\hbar k}\right) \sin\left(\frac{m\Omega'l}{2\hbar k}\right) \right]^2. \quad (2)$$

However, if the kinetic energy of the atom is comparable with the interaction energy, the semiclassical approach is not valid anymore and a full quantum mechanical solution is required.

### 3 Quantum treatment

For the given initial value problem of a left incoming ground-state plane wave the asymptotic solution of the SSE to the right of the laser fields is given by

$$\Phi_k(x) = \frac{1}{\sqrt{2\pi}}(T_{11}^1 e^{ikx}|1\rangle + T_{12}^1 e^{iqx}|2\rangle), \quad x \geq 2l + L, \quad (3)$$

where  $T_{11}^1$  ( $T_{12}^1$ ) is the transmission amplitude for the ground (excited) state.

From equation (3) one sees that after passing the two laser fields, the atom will either be still in the ground state, propagating with wavenumber  $k$  or in the excited state, propagating with wavenumber  $q = \sqrt{k^2 + 2m\Delta/\hbar}$ . In the latter case, the atomic transition  $|1\rangle \rightarrow |2\rangle$  induced by the laser field is responsible for a change of kinetic energy [6]. For  $\Delta > 0$  the kinetic energy of the excited state component has been enhanced by  $\hbar\Delta$  whereas for  $\Delta < 0$  the kinetic energy has been reduced by  $\hbar\Delta$  and the laser will slow down the atom. For  $\Delta$  smaller than the

critical value  $\Delta_{\text{cr}} = -\hbar k^2/2m$ , the excited state component becomes evanescent and its transmission probability vanishes (closed channel). Thus, the quantum mechanical probability to observe the transmitted atom in the excited state is zero for  $\Delta \leq \Delta_{\text{cr}}$  and

$$P_{12} = \frac{q}{k} |T_{12}^1|^2 \quad \text{for } \Delta > \Delta_{\text{cr}}. \quad (4)$$

#### 3.1 Two-channel recurrence relations

In the following, we generalise the well-known recurrence relations for one-channel scattering [11] to the two-channel case. This allows us to express the double-barrier scattering amplitudes and in particular  $T_{12}^1$  in terms of the single-barrier ones. First we will give the eigenstates of  $H$  within a constant potential region and match them at the boundaries. Note that for the nonresonant case it is not possible to find a dressed state basis that diagonalises  $H$  on the whole axis [6]. Outside the laser fields (regions  $m = 0, 2, 4$ , see Fig. 1) the general solution of the SSE is

$$\Phi_k^{(m)}(x) = \frac{1}{\sqrt{2\pi}} \left( (A_m^+ e^{ikx} + B_m^+ e^{-ikx})|1\rangle + (A_m^- e^{iqx} + B_m^- e^{-iqx})|2\rangle \right). \quad (5)$$

Within a laser barrier the (unnormalised) dressed state basis that diagonalises the Hamiltonian is given by  $|\lambda_{\pm}\rangle = |1\rangle + 2\lambda_{\pm}\Omega^{-1}|2\rangle$  where  $\lambda_{\pm} = (-\Delta \pm \Omega')/2$  are the dressed eigenvalues. Thus, the solutions in the interaction regions ( $m = 1, 3$ ) are of the form

$$\Phi_k^{(m)}(x) = \frac{1}{\sqrt{2\pi}} \left( A_m^+ |\lambda_+\rangle e^{ik+x} + B_m^+ |\lambda_+\rangle e^{-ik+x} + A_m^- |\lambda_-\rangle e^{ik-x} + B_m^- |\lambda_-\rangle e^{-ik-x} \right) \quad (6)$$

with wavenumbers  $k_{\pm}^2 = k^2 - 2m\lambda_{\pm}/\hbar$ . For the matching conditions it is convenient to use a two-channel transfer matrix formalism [10]. For this we define the column vectors  $\mathbf{v}_m = (A_m^+, B_m^+, A_m^-, B_m^-)^T$ ,  $m = 0, \dots, 4$ , and the matching matrices  $\mathbf{M}_0(x)$  and  $\mathbf{M}_b(x)$ , such that the usual matching conditions between the free region and the barrier region at position  $x_1$  are given by  $\mathbf{M}_0(x_1)\mathbf{v}_m = \mathbf{M}_b(x_1)\mathbf{v}_{m+1}$  and between barrier region and free region at position  $x_2$  by  $\mathbf{M}_b(x_2)\mathbf{v}_m = \mathbf{M}_0(x_2)\mathbf{v}_{m+1}$ . The matrices  $\mathbf{M}_0(x)$  and  $\mathbf{M}_b(x)$  are given explicitly in reference [10]. Then the matching conditions between the regions  $m = 0$  and  $m = 2$  and between regions  $m = 0$  and  $m = 4$  read  $\mathbf{v}_0 = \boldsymbol{\alpha} \cdot \mathbf{v}_2 = \boldsymbol{\alpha}\tilde{\boldsymbol{\alpha}} \cdot \mathbf{v}_4$ , where  $\boldsymbol{\alpha} = \mathbf{M}_0^{-1}(0)\mathbf{M}_b(0)\mathbf{M}_b^{-1}(l)\mathbf{M}_0(l)$  and  $\tilde{\boldsymbol{\alpha}} = \mathbf{M}_0^{-1}(l+L)\mathbf{M}_b(l+L)\mathbf{M}_b^{-1}(2l+L)\mathbf{M}_0(2l+L)$ . Therefore, the scattering amplitudes of the single-barrier problem are given in terms of the  $\alpha_{ij}$  for any initial value problem. We denote in the following by  $r_{ij}^1(t_{ij}^1)$ ,  $i, j = 1, 2$ , the single-laser reflection (transmission) amplitude for incidence from the left in the  $i$ th channel and an outgoing plane wave in the  $j$ th channel, and by  $r_{ij}^r$  and  $t_{ij}^r$  the corresponding amplitudes for right incidence. The corresponding quantities for

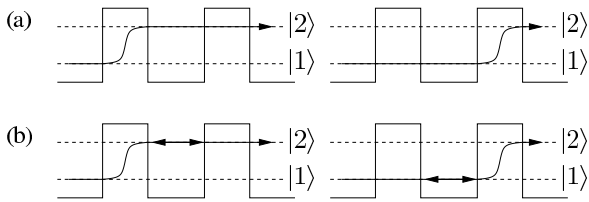


**Fig. 2.** (a) Leading order contribution to the scattering paths for the direct scattering regime. (b) Leading order contributions to the scattering paths for the multiple scattering regime (Fabry-Perot).

the second laser barrier will differ only by a phase factor and they are denoted by a tilde,  $\tilde{r}_{ij}^{l,r}, \tilde{t}_{ij}^{l,r}$ . One can show that the relation between the 16 scattering amplitudes  $r_{ij}^{l,r}, t_{ij}^{l,r}$  and the  $\alpha_{ij}$  is invertible, thus  $\alpha_{ij} = f(r_{ij}^{l,r}, t_{ij}^{l,r})$  and  $\tilde{\alpha}_{ij} = g(\tilde{r}_{ij}^{l,r}, \tilde{t}_{ij}^{l,r})$  with known functions  $f$  and  $g$ . Since the scattering amplitudes of the double-barrier problem are given in terms of  $\alpha_{ij}$  and  $\tilde{\alpha}_{ij}$ , this shows the desired connection between single barrier and double barrier case. In particular, one obtains

$$T_{12}^l = \left[ t_{12}^l \tilde{t}_{22}^l + t_{11}^l \tilde{t}_{12}^l - (r_{12}^r t_{11}^l - r_{11}^r t_{12}^l)(\tilde{r}_{21}^l \tilde{t}_{12}^l - \tilde{r}_{11}^l \tilde{t}_{22}^l) + (r_{22}^r t_{11}^l - r_{21}^r t_{12}^l)(\tilde{r}_{22}^l \tilde{t}_{12}^l - \tilde{r}_{12}^l \tilde{t}_{22}^l) \right] \times \left[ 1 - r_{12}^r \tilde{r}_{21}^l - r_{22}^r \tilde{r}_{22}^l - r_{11}^r \tilde{r}_{11}^l - r_{21}^r \tilde{r}_{12}^l - (r_{12}^r r_{21}^l - r_{22}^r r_{11}^l)(\tilde{r}_{11}^l \tilde{r}_{22}^l - \tilde{r}_{21}^l \tilde{r}_{12}^l) \right]^{-1}. \quad (7)$$

Note that this result is valid for arbitrary laser intensity profiles. We will show in the following that a clear physical interpretation of equation (7) can be given within a multiple scattering picture.

### 3.2 Direct scattering regime

If the kinetic energy is larger than the Rabi energy the scattering process will be dominated by transmission through both laser barriers. Thus, one has  $|t_{ij}^{l,r}| \gg |r_{ij}^{l,r}|$  and expanding the denominator of equation (7) yields

$$T_{12}^l = (t_{11}^l \tilde{t}_{12}^l + t_{12}^l \tilde{t}_{22}^l) + (t_{12}^l (\tilde{r}_{21}^l r_{11}^r + \tilde{r}_{22}^l r_{21}^r) \tilde{t}_{12}^l + t_{11}^l (\tilde{r}_{11}^l r_{12}^r + \tilde{r}_{12}^l r_{22}^r) \tilde{t}_{22}^l + t_{12}^l (\tilde{r}_{21}^l r_{12}^r + \tilde{r}_{22}^l r_{22}^r) \tilde{t}_{22}^l + t_{11}^l (\tilde{r}_{11}^l r_{11}^r + \tilde{r}_{12}^l r_{21}^r) \tilde{t}_{12}^l) + \dots \quad (8)$$

The two terms in the first bracket of this expansion describe the direct scattering process (Fig. 2a) whereas the second bracket contains all possible paths to first order of multiple scatterings including two reflections.

Keeping only the two direct scattering paths and using  $\tilde{t}_{22}^l = t_{22}^l$  and  $\tilde{t}_{12}^l = t_{12}^l \exp[i(k-q)(l+L)]$  leads to

$$P_{12} = \frac{q}{k} |t_{12}^l|^2 \left| t_{22}^l + t_{11}^l e^{i(k-q)(l+L)} \right|^2. \quad (9)$$

This expression describes interferences between atoms which pass the first laser in the ground state and are excited in the second laser and atoms which are excited in

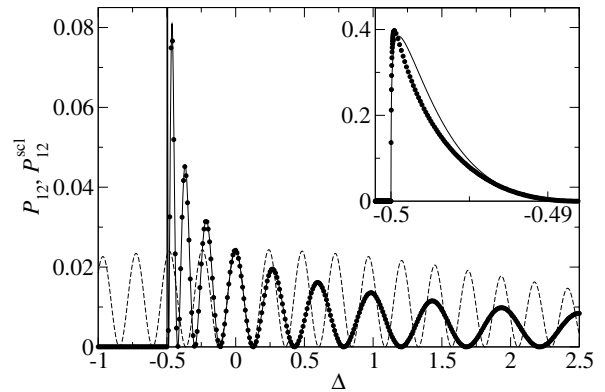


**Fig. 3.** The detection probability  $P_{12}$  with respect to  $\Delta$  in the direct scattering regime ( $E_k \gg \hbar\Omega$ ). Comparison of exact result obtained with equation (7) (solid line), direct scattering approximation (9) (circles) and semiclassical result  $P_{12}^{scl}$  (dashed line) for  $k = 1$ ,  $\Omega = \pi/20$ ,  $l = 1$ ,  $L = 25$ . The inset shows a closeup of the peak close to  $\Delta_{cr}$ . For plots we use dimensionless units with  $\hbar = m = 1$ .

the first laser and pass the second one in the excited state. However, we emphasise the fact that equation (9) goes beyond the validity of the semiclassical expression (2) since  $E_k$  has not to be large with respect to  $\hbar\Delta$  and the overall transmission probability might be smaller than one.

The explicit expressions for the single-barrier amplitudes are  $t_{11}^l = -\alpha_{33}/d_\alpha$ ,  $t_{12}^l = \alpha_{31}/d_\alpha$  and  $t_{22}^l = -\alpha_{11}/d_\alpha$  where  $d_\alpha = \alpha_{13}\alpha_{31} - \alpha_{11}\alpha_{33}$  and

$$\alpha_{11} = e^{ikl} [\lambda_+ d_-(k, k) - \lambda_- d_+(k, k)] / \Omega',$$

$$\alpha_{31} = \frac{1}{4} \Omega e^{ikl} \left[ d_+(k, q) - d_-(k, q) + \frac{k}{q} (d_+(q, k) - d_-(q, k)) \right] / \Omega',$$

$$\alpha_{13} = \alpha_{31}(k \leftrightarrow q), \quad \alpha_{33} = \alpha_{11}(k \rightarrow q, d_+ \leftrightarrow d_-),$$

$$d_\pm(k_1, k_2) = \cos(k_\pm l) - \sigma_\pm(k_1, k_2) \sin(k_\pm l),$$

$$\sigma_\pm(k_1, k_2) = i(k_1/k_\pm + k_\pm/k_2)/2. \quad (10)$$

The given replacement rules apply only to the exponents and arguments and not to the indirect dependencies within the  $k_\pm$ . Expanding  $P_{12}$  with respect to  $k \rightarrow \infty$  gives back the semiclassical result (2), as expected.

Figure 3 illustrates the behaviour of  $P_{12}$  as a function of  $\Delta$ . For comparison we have plotted the exact result obtained by means of equations (7) and the semiclassical expression  $P_{12}^{scl}$ . For  $E_k/\hbar\Omega \approx 3.2$  the agreement between  $P_{12}$  and the exact result is very good and becomes even better for larger velocities. Thus, the scattering process is dominated by the two paths shown in Figure 2a. Nevertheless, one sees that the interference pattern can not be understood within the semiclassical approximation for  $\hbar|\Delta| \gtrsim E_k$ . For  $\Delta > 0$ , the zeros of the interference pattern become dispersed with respect to  $P_{12}^{scl}$  whereas for  $\Delta_{cr} < \Delta < 0$  the fringes become closer and narrower up to extremely narrow peaks close to  $\Delta_{cr}$  (see inset of Fig. 3). Physically, this is related to the discussion below equation (3). For negative detuning and close to

the critical value the excited atom has been slowed down and the effective crossing time scale  $t_{\text{eff}} = mL/\hbar q$  will be much larger than the semiclassical crossing time scale  $t_{\text{scl}} = mL/\hbar k$ . This produces a finite number of peaks in the negative detuning region. On the other hand, for positive detuning the atom is sped up and  $t_{\text{eff}} < t_{\text{scl}}$ , leading to a broader interference pattern. As the critical detuning depends on the atomic momentum, it may be difficult to use the narrowing effect for metrological purposes. For current experiments the region close to  $\Delta = 0$  where the semiclassical condition is satisfied contains much more fringes than shown in Figure 3.

### 3.3 Multiple scattering regime

Let us now consider the opposite regime, where the kinetic energy of the atom is much smaller than the Rabi energy. In this case one has  $|r_{12}^{\text{r}}, |r_{21}^{\text{r}}, |t_{ij}^{\text{r}}| \ll |r_{11}^{\text{r}}, |r_{22}^{\text{r}}|$ . We checked explicitly that the leading order of the small scattering amplitudes is  $(E_k/\hbar\Omega)^{1/2}$ , respectively, whereas the leading order of  $r_{11}^{\text{r}}$  and  $r_{22}^{\text{r}}$  is 1. Thus, an expansion of  $T_{12}^{\text{l}}$  in a series with respect to powers of the small amplitudes yields

$$T_{12}^{\text{l}} = \frac{t_{12}^{\text{l}}\tilde{t}_{22}^{\text{l}}}{1 - r_{22}^{\text{r}}\tilde{r}_{22}^{\text{l}}} + \frac{t_{11}^{\text{l}}\tilde{t}_{12}^{\text{l}}}{1 - r_{11}^{\text{r}}\tilde{r}_{11}^{\text{l}}} + \frac{t_{11}^{\text{l}}\tilde{t}_{22}^{\text{l}}(r_{12}^{\text{r}}\tilde{r}_{11}^{\text{l}} + r_{22}^{\text{r}}\tilde{r}_{12}^{\text{l}})}{(1 - r_{11}^{\text{r}}\tilde{r}_{11}^{\text{l}})(1 - r_{22}^{\text{r}}\tilde{r}_{22}^{\text{l}})} + \frac{t_{12}^{\text{l}}\tilde{t}_{12}^{\text{l}}(r_{11}^{\text{r}}\tilde{r}_{21}^{\text{l}} + r_{22}^{\text{r}}\tilde{r}_{22}^{\text{l}})}{(1 - r_{11}^{\text{r}}\tilde{r}_{11}^{\text{l}})(1 - r_{22}^{\text{r}}\tilde{r}_{22}^{\text{l}})} + \dots, \quad (11)$$

where the first two terms contain second powers of the small scattering amplitudes, the next given terms contain third powers and so on. Again, these terms can be given a clear physical interpretation in terms of multiple scatterings. The first two terms correspond to two families of paths, the first of which describes atoms being excited in the first laser and cross the second laser in the excited state after multiple internal reflections, whereas the second family corresponds to atoms crossing the first barrier in the ground state, which undergo multiple internal reflections in the ground state and are finally excited in the second laser (Fig. 2b). Similarly, the following terms account for all possible paths with exactly one internal excitation by means of reflection. Keeping only the leading order of equation (11) and using  $r_{22}^{\text{r}} = r_{22}^{\text{l}} \exp(-2iqL)$  and  $r_{11}^{\text{r}} = r_{11}^{\text{l}} \exp(-2ikL)$ , the probability to observe an outgoing atom in the excited state is

$$P_{12} = \frac{q}{k} \left| \frac{t_{12}^{\text{l}}t_{22}^{\text{l}}}{1 - (r_{22}^{\text{l}})^2 e^{2iqL}} + \frac{t_{11}^{\text{l}}t_{12}^{\text{l}} e^{i(k-q)(l+L)}}{1 - (r_{11}^{\text{l}})^2 e^{2ikL}} \right|^2. \quad (12)$$

Again, we give explicit analytical results by writing the scattering coefficients in terms of the  $\alpha_{ij}$ . We find  $r_{11}^{\text{l}} = (\alpha_{23}\alpha_{31} - \alpha_{21}\alpha_{33})/d_\alpha$  and  $r_{22}^{\text{l}} = (\alpha_{41}\alpha_{13} - \alpha_{43}\alpha_{11})/d_\alpha$  where

$$\begin{aligned} \alpha_{41} &= \alpha_{31}(q \rightarrow -q), & \alpha_{23} &= \alpha_{13}(k \rightarrow -k), \\ \alpha_{21} &= e^{ikl} [\lambda_- \sigma_+(k, -k) \sin(k_+ l) \\ &\quad - \lambda_+ \sigma_-(k, -k) \sin(k_- l)] / \Omega', \\ \alpha_{43} &= \alpha_{21}(k \rightarrow q, \sigma_+ \leftrightarrow \sigma_-). \end{aligned} \quad (13)$$

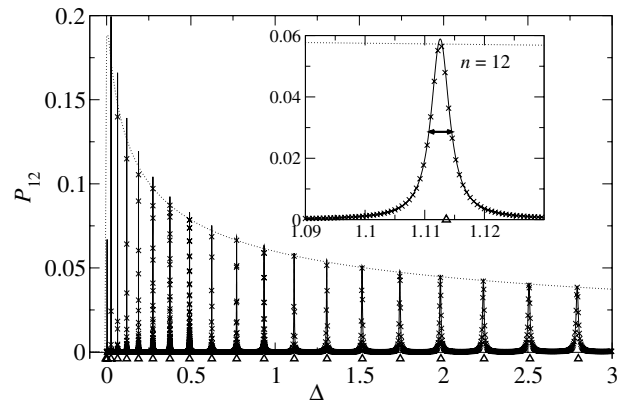


**Fig. 4.** The detection probability  $P_{12}$  with respect to  $\Delta$  in the multiple-scattering regime. Comparison of the exact result obtained with equation (7) (solid line) and the approximation (12) (crosses) for  $k = 0.1$ ,  $\Omega = 15\pi$ ,  $l = 1.2$ ,  $L = 25$ . The envelope (dotted line), the resonance positions (triangles) and its width are in good agreement with the exact result. The inset shows a closeup of the 12th resonance.

For the resonant case,  $\Delta = 0$ , we obtain  $t_{11}^{\text{l}} = t_{22}^{\text{l}} = (\tau_+ + \tau_-)/2$ ,  $t_{12}^{\text{l}} = (\tau_+ - \tau_-)/2$ ,  $r_{11}^{\text{l}} = r_{22}^{\text{l}} = (\rho_+ + \rho_-)/2$  and  $P_{12}$  can be written in terms of the one-channel double barrier and double well amplitudes  $\tau_\pm$  and  $\rho_\pm$  given in reference [5].

Equation (12) may be understood as a coherent sum of two Fabry-Perot-like terms. Both of them exhibit resonances with respect to  $k$ , but only the first one shows resonances with respect to  $\Delta$ . The reason is that only the excited state sums up a  $\Delta$ -dependent phase while crossing the intermediate region. Therefore the second term in equation (12) can be omitted for  $k \neq n\pi/L$  and the remaining term can be written as  $P_{12} = A/[1 + F^2 \sin^2(qL + \varphi)]$ , where  $A = q|t_{12}^{\text{l}}t_{22}^{\text{l}}|^2/[k(1 - |r_{22}^{\text{l}}|^2)^2]$  is the envelope and  $F = 2|r_{22}^{\text{l}}|/(1 - |r_{22}^{\text{l}}|^2)$  the finesse of the Fabry-Perot pattern and  $r_{22}^{\text{l}} = |r_{22}^{\text{l}}| \exp(i\varphi)$ . From this one obtains the positions of the resonances in leading order,  $r_{22}^{\text{l}} \approx -1$ , to be at  $\Delta_n = \Delta_{\text{cr}} + \hbar n^2 \pi^2 / (2mL)^2$ ,  $n = 1, 2, 3, \dots$  and its widths to be  $w_\Delta = 2n\pi\hbar(mL^2)^{-1}(1 - |r_{22}^{\text{l}}|)^2|_{\Delta=\Delta_n}$ . A typical picture is given in Figure 4, where  $P_{12}$  is plotted for  $E_k/\hbar\Omega \approx 10^{-4}$ . With this ratio, it can be seen that equation (12) as well as the envelope, the resonance positions and widths are in good agreement with the exact result.

## 4 Discussion

We have studied analytically the behaviour of Ramsey fringes including quantum reflections from the fields. Due to the recent progress in atom cooling, wave guide and atom chip technology and mazer physics this is a timely investigation. By means of two-channel recurrence relations we have identified the dominant contributions to the scattering process in the direct scattering regime and in the multiple-scattering regime. We have shown that for  $E_k \gg \hbar\Omega$  the interference fringes for negative detuning are narrower than the prediction of semiclassical theory.

For very slow atoms,  $E_k \ll \hbar\Omega$ , interference is completely suppressed and the transmission probability is dominated by scattering resonances, leading to a matter-wave Fabry-Perot device.

The methods of the current work can easily be adopted to quantised fields to describe the passage of ultracold atoms through two microwave high-Q cavities. For example, it would be interesting to study if and how quantised motion affects the recent results for the dependence of the fringes on quantum statistics of the fields [12].

This work has been supported by Ministerio de Educación y Ciencia (BFM2003-01003) and UPV-EHU (00039.310-15968-/2004). D.S. acknowledges a fellowship within the Postdoc-Programme of the German Academic Exchange Service (DAAD).

## References

1. N.F. Ramsey, Phys. Rev. **78**, 695 (1950); N.F. Ramsey, *Molecular beams* (Clarendon Press, Oxford, 1956)
2. Ph. Laurent et al., Eur. Phys. J. D **3**, 201 (1998); Ch. Salomon et al., C. R. Acad. Sci. Paris Série IV **2**, 1313 (2001)
3. C.J. Bordé, C. R. Acad. Sci. Paris Série IV **2**, 509 (2001); P. Wolf et al., *Recoil Effects in Microwave Atomic Frequency Standards: an update*, in *Proc. 6th Symp. on Frequency Standards and Metrology*, edited by P. Gill (World Scientific, 2002), p. 593; C.J. Bordé, Metrologia **39**, 435 (2002)
4. B.-G. Englert, J. Schwinger, A.O. Barut, M.O. Scully, Europhys. Lett. **14**, 25 (1991); M.O. Scully, G.M. Meyer, H. Walther, Phys. Rev. Lett. **76**, 4144 (1996)
5. G.S. Agarwal, R. Arun, Phys. Rev. Lett. **84**, 5098 (2000); R. Arun, G.S. Agarwal, Phys. Rev. A **64**, 065802 (2001)
6. T. Bastin, J. Martin, Phys. Rev. A **67**, 053804 (2003)
7. Ch.J. Bordé et al., Phys. Rev. A **30**, 1836 (1984)
8. J.H. Thywissen et al., Eur. Phys. J. D **7**, 361 (1999)
9. I. Lizuain, A. Ruschhaupt, J.G. Muga, preprint (2006) [arXiv:quant-ph/0602013](https://arxiv.org/abs/quant-ph/0602013)
10. J.A. Damborenea, I.L. Egusquiza, G.C. Hegerfeldt, J.G. Muga, J. Phys. B: At. Mol. Opt. Phys. **36**, 2657 (2003); note the typo in equation (A.2) where the factors  $2\lambda_{\pm}/\Omega$  are missing in the second and fourth row
11. M.G. Rozman, P. Reineker, R. Tehver, Phys. Rev. A **49**, 3310 (1994)
12. G.S. Agarwal, P.K. Pathak, M.O. Scully, Phys. Rev. A **67**, 043807 (2003)